Aalborg Universitet

Ping-Pong Beam Training with Hybrid Digital-Analog Antenna Arrays

Manchón, Carles Navarro; Carvalho, Elisabeth De; Andersen, Jørgen Bach

Ping-Pong Beam Training with Hybrid Digital-Analog Antenna Arrays

Carles Navarro Manchón, Elisabeth de Carvalho, and Jørgen Bach Andersen

Department of Electronic Systems, Aalborg University, Denmark

Email: {cnm, edc, jba}@es.aau.dk

Abstract—In this article we propose an iterative training scheme that approximates optimal beamforming between two transceivers equipped with hybrid digital-analog antenna arrays. Inspired by methods proposed for digital arrays that exploit algebraic power iterations, the proposed training procedure is based on a series of alternate (ping-pong) transmissions between the two devices over a reciprocal channel. During the transmissions, the devices update their digital beamformers by conjugation and normalization operations on the received digital signal, while the analog beamformers are progressively updated by a simple "beam split and drop" strategy that tracks the directions from which signals with largest magnitude are being received. The resulting scheme has minimal computational complexity and converges with only a handful of iterations. As shown in the numerical assessment, the method approximates the top singular mode of the channel, hence performing very closely to optimal beamforming.

I. Introduction

Wireless communication systems employing large carrier frequencies enable the implementation of antenna arrays with a large number of elements, as the physical size of the array is proportional to the carrier wavelength. This aspect, together with the saturation of the wireless spectrum below 6 GHz, have directed the attention of researchers towards the frequency bands in the range of 30–300 GHz as candidate bands for the development of 5th generation (5G) cellular systems [1], [2]. It is expected that the beamforming gains that can be obtained with large antenna arrays will compensate for the large free-space propagation losses at these frequencies. Wireless communication systems operating in these bands are usually encompassed under the umbrella of millimeter-wave (mmWave) communication systems.

Although the use of mmWave bands makes it feasible to design antenna arrays with very large number of elements and a small physical size –such that they can be used in small devices– it also entails some challenges. First, the close spacing between antennas makes it hard to implement all the circuitry necessary to digitally control each of the antenna elements. Second, even if the physical implementation was possible, the power consumption associated with the digital signal processing needed for such large number of elements becomes prohibitive [3]. A promising architecture to alleviate these drawbacks is that of a hybrid digital-analog antenna array [4], [5]. In hybrid antenna arrays, a small number of radio-frequency (RF) chains are connected to a network of phase shifters that perform beamforming/combining in the analog domain, as illustrated in Fig. 1. While this architecture

has clear advantages in terms of cost and power consumption, it complicates the acquisition of channel state information (CSI) and the processing needed to compute beamformers and/or precoders, as we discuss next.

There are two main obstacles for the acquisition of CSI in systems with large hybrid antenna arrays at both ends. On the one hand, the large dimensionality of the channel matrix implies that long training sequences are needed, which is further aggravated in the mmWave case due to the low SNR resulting from high propagation losses. On the other hand, the fact that the MIMO channel matrix is not directly observable, but is instead observed only after analog precoding and combining, prohibits the use of typical estimators used with fully digital arrays. Nonetheless, the assumed sparse nature of mmWave channels has enabled the proposal of compressed-sensing based solutions, as in [6], [7]. The proposed approaches, however, still involve significant complexity and latency. A simpler alternative is that of beam search protocols [8], [9]. In beam search protocols, the involved devices align their beamformers by means of a (possibly hierarchical) search over directional beams in a predefined codebook. To enable the beam search, the devices need to scan transmission and reception over the different beams in the codebook, which may imply significant latency. Beam search protocols have the advantage of simplicity, at the cost of a suboptimal beamformer alignment. Beamforming performance can be improved by using larger codebooks with better spatial resolution at the expense of further latency due to the search procedures.

Here, however, we focus on a different beam training strategy: ping-pong beam training (PPBT). The core of the idea was first sketched for digital arrays in [10], [11] and recently extended to systems involving large antenna arrays and frequency-selective channels in [12]. PPBT relies on alternate transmissions through a reciprocal channel in which each device simply conjugates and normalizes its received signal before transmitting it back to the other device. The sequence of transmissions inherently implements an algebraic power iteration that converges to the right and left singular vectors associated to the maximum singular value of the channel matrix. The principle was extended to spatial multiplexing MIMO in [13], which has in turn inspired a related proposal for mmWave systems [14].

In this article, we present a PPBT approach that estimates the top singular mode of reciprocal MIMO channels between
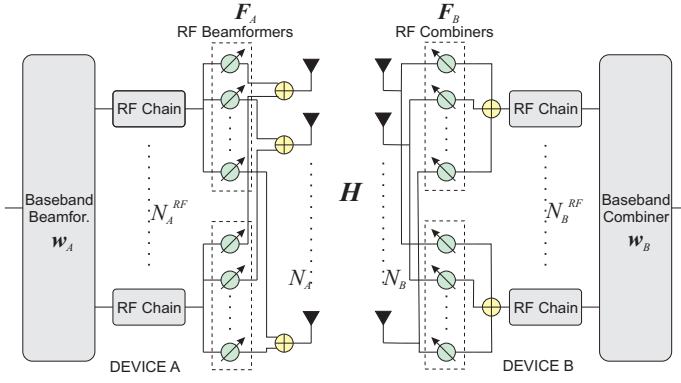
Fig. 1. Hybrid Digital-Analog Antenna Arrays.

two devices equipped with hybrid antenna arrays, which we coin *hybrid PPBT*. To enable the use of PPBT with hybrid arrays, we include an algorithm that progressively chooses the analog beamformers at each device from a predefined hierarchical codebook. Starting with beams of maximal width, the purpose of the algorithm is to steer beams that are more and more directive (thinner beams) towards the directions where most signal power is received, in order to maximize the chance to align the most directive beams with the strongest channel multipath components. After one round-trip transmission, the received power in each beam is measured. The beam with largest power is replaced by two more directive beams while the beam with smaller power is deleted, in order to keep the number of simultaneously active analog beams equal to the number of RF chains. We call this strategy "beam split and drop". At the same time, the digital beamformers are updated via conjugation and normalization operations on the received signal, as in the digital PPBT. As illustrated in the numerical results, our proposed scheme performs very closely to optimal beamforming for moderate and high signal-to-noise ratios (SNR), while being much more robust than PPBT algorithms using digital arrays at low SNRs. The robustness of our proposed method against low SNR conditions prior to beam alignment makes it especially suitable for mmWave communications. In comparison to the approach in [14], hybrid PPBT is much simpler in terms of computational complexity and requires significantly less training data.

II. SYSTEM MODEL

We consider a system consisting of two transceivers A and B that exchange single-layer transmissions over a reciprocal MIMO channel. Transceiver A (B) is equipped with a hybrid, uniform linear antenna array consisting of N_A (N_B) isotropic antennas, with inter-element distance $d = \lambda/2$, with λ denoting the wavelength. The array is controlled by N_A^{RF} (N_B^{RF}) RF chains whose input can be digitally modulated, and which are each connected to a set of analog phase shifters, as illustrated by Fig. 1.

With the system configuration described above, a training sequence is transmitted by device A. The purpose of the training sequence is to estimate the useful part in the received

signal, i.e. vector $\boldsymbol{F}_B^{\mathrm{T}} \boldsymbol{H} \boldsymbol{F}_A \boldsymbol{w}_A$ as defined below, and average out the noise. Once conjugated and normalized, the estimate serves as the digital beamforming vector for transmission. After the processing required by least-squares training-based estimation, the received signal is

$$\boldsymbol{y}_B = \boldsymbol{F}_B^{\mathrm{T}} \boldsymbol{H} \boldsymbol{F}_A \boldsymbol{w}_A + \boldsymbol{F}_B^{\mathrm{T}} \boldsymbol{n}_B \quad (1)$$

where $\boldsymbol{H} \in \mathbb{C}^{N_B \times N_A}$ denotes the MIMO channel matrix, $\boldsymbol{F}_A \in \mathbb{C}^{N_A \times N_A^{RF}}$ and $\boldsymbol{F}_B \in \mathbb{C}^{N_B \times N_B^{RF}}$ contain the states of the analog precoder and combiner of transceivers A and B, $\boldsymbol{w}_A \in \mathbb{C}^{N_A^{RF}}$ denotes the digital precoder of transceiver A, and $\boldsymbol{n}_B \in \mathbb{C}^{N_B}$ is a complex, circularly-symmetric AWGN vector with variance σ^2. We stress that $\boldsymbol{n}_B$ denotes the equivalent noise vector resulting from last-squares training processing. Since we assume channel reciprocity, the equivalent signal received by device A after a training transmission by device B and corresponding receive processing reads

$$\boldsymbol{y}_A = \boldsymbol{F}_A^{\mathrm{T}} \boldsymbol{H}^{\mathrm{T}} \boldsymbol{F}_B \boldsymbol{w}_B + \boldsymbol{F}_A^{\mathrm{T}} \boldsymbol{n}_A \quad (2)$$

with $\boldsymbol{w}_B \in \mathbb{C}^{N_B^{RF}}$ denoting the digital precoder of transceiver B and $\boldsymbol{n}_A \in \mathbb{C}^{N_A}$ being again a complex, circularly-symmetric AWGN vector with variance σ^2.

We assume a finite scatterer channel model with P propagation paths. Hence, the channel matrix can be expressed as [15]

$$\boldsymbol{H} = \sqrt{\frac{N_A N_B}{P}} \sum_{p=1}^{P} \alpha_p \boldsymbol{a}_B(\Omega_{B,p}) \boldsymbol{a}_A^{\mathrm{T}}(\Omega_{A,p}) \quad (3)$$

where α_p are independent, standard complex Gaussian variables denoting the gain of the pth multipath component between the first elements of the transmit and receive arrays; $\boldsymbol{a}_A(\Omega_{A,p}) = [1, e^{-j\Omega_{A,p}}, \ldots, e^{-j(N_A-1)\Omega_{A,p}}]^{\mathrm{T}}/\sqrt{N_A}$ and $\boldsymbol{a}_B(\Omega_{B,p}) = [1, e^{-j\Omega_{B,p}}, \ldots, e^{-j(N_B-1)\Omega_{B,p}}]^{\mathrm{T}}/\sqrt{N_B}$ are the steering vectors of the pth path between arrays A and B; $\Omega_{A,p} = 2\pi d \cos(\theta_{A,p})/\lambda = \pi \cos(\theta_{A,p})$ and $\Omega_{B,p} = 2\pi d \cos(\theta_{B,p})/\lambda = \pi \cos(\theta_{B,p})$ are the directional cosines corresponding to the pth path at arrays A and B; finally, $\theta_{A,p}$ and $\theta_{B,p}$ are the angles of incidence of the pth propagation path at arrays A and B, which are uniformly distributed in the range $[0, 2\pi)$ radians. The geometric modeling in (3) will be exploited in the ping-pong beamforming algorithm to set the analog precoders $\boldsymbol{F}_A$ and $\boldsymbol{F}_B$, as will be detailed in the following section.

III. PROPOSED TRAINING WITH HYBRID ARRAYS

The analog precoders $\boldsymbol{F}_A, \boldsymbol{F}_B$ and digital precoders $\boldsymbol{w}_A, \boldsymbol{w}_B$ fulfill some constraints due to the hybrid array structure employed. Firstly, we impose a power normalization constraint on the effective precoders such that $\|\boldsymbol{F}_A \boldsymbol{w}_A\|_2^2 = \|\boldsymbol{F}_B \boldsymbol{w}_B\|_2^2 = 1$. Secondly, since the entries of the analog precoding matrices $\boldsymbol{F}_A, \boldsymbol{F}_B$ represent the operation of analog phase shifters, they fulfill $\boldsymbol{F}_A[m,n], \boldsymbol{F}_B[m',n'] \in \{0\} \cup \{e^{j\phi} : \phi \in [0, 2\pi)\}$. The case $\boldsymbol{F}_A[m,n] = 0$ accounts for the situation in which the mth array element of transceiver A is left unused by the nth RF chain.

Subject to these constraints, transceivers A and B must select their analog and digital precoders to optimize a given objective function. As we only consider single layer transmission in this work, we select as objective function the beamforming gain[1], defined as

$$G = \left| \boldsymbol{w}_B^{\mathrm{T}} \boldsymbol{F}_B^{\mathrm{T}} \boldsymbol{H} \boldsymbol{F}_A \boldsymbol{w}_A \right|^2. \tag{4}$$

The precoders that maximize the above gain are well-known to be $\boldsymbol{F}_A \boldsymbol{w}_A = \boldsymbol{v}_{max}$ and $\boldsymbol{F}_B \boldsymbol{w}_B = \boldsymbol{u}_{max}^*$, where $\boldsymbol{v}_{max}$ and $\boldsymbol{u}_{max}$ denote respectively the right and left singular vectors of matrix $\boldsymbol{H}$ associated to its maximum singular value λ_{max}. This solution leads to the optimal beamforming gain $G_{opt} = \lambda_{max}^2$, as transmission is performed over the top singular mode of the channel. The optimal beamformers $\boldsymbol{v}_{max}$ and $\boldsymbol{u}_{max}^*$ can be computed by performing a (computationally costly) singular value decomposition of the MIMO channel matrix, but this requires full knowledge of $\boldsymbol{H}$.

In order to circumvent the estimation of the channel matrix $\boldsymbol{H}$, we propose a beam training procedure based on alternating transmissions between the two devices in such a way that the digital and analog precoders approximate the optimal beamformers without explicit channel estimation. The proposed procedure mainly consists of two parts: 1) a "beam split and drop" approach to select the analog precoders $\boldsymbol{F}_A$ and $\boldsymbol{F}_B$ from predefined multilevel codebooks, and 2) a method to select the digital beamformers $\boldsymbol{w}_A$ and $\boldsymbol{w}_B$ inspired by the digital beam-training procedure in [12]. In the following, we shortly review the beam training procedure for digital antenna arrays, then present the proposed codebook for the analog precoders, and our proposed beam-training solution.

A. Ping-Pong Beam Training with Digital Antenna Arrays

We review the digital PPBT algorithm over a narrowband reciprocal channel $\boldsymbol{H}$ as described in [12]. We consider two devices A and B equipped with digitally controlled antenna arrays with N_A and N_B elements respectively. At the initial (0th) iteration, the process starts with a random initialization of the beamforming vector at device A, $\boldsymbol{w}_A^{[0]}$. With this, device A transmits a training sequence to device B. Based on the training sequence, device A gets an estimate of $\boldsymbol{H} \boldsymbol{w}_A^{[0]}$, then conjugates and normalizes it. The result is used as the beamforming vector $\boldsymbol{w}_B^{[0]}$ to transmit a training sequence back to device A, who repeats the same operations. This process is reiterated until convergence.

There are 2 parallel iteration sets: one set for device A based on composite channel $\boldsymbol{H}^{\mathrm{H}} \boldsymbol{H}$ and one set for device B based on composite channel $\boldsymbol{H}^* \boldsymbol{H}^{\mathrm{T}}$. Each set corresponds to a separate power iteration algorithm [16]: one computing the max-eigenvector of $\boldsymbol{H}^{\mathrm{H}} \boldsymbol{H}$ and the other one the max-eigenvector of $\boldsymbol{H}^* \boldsymbol{H}^{\mathrm{T}}$. At device A, the algorithm converges to the right max-singular vector of $\boldsymbol{H}$. At device B, the algorithm converges to the right max-singular vector of $\boldsymbol{H}^{\mathrm{T}}$. Further details, including an analysis of the perturbation introduced by noise, can be found in [12].

B. Analog Precoder Codebooks

The codebook[2] is implemented so that the columns $\boldsymbol{f}_{A,i}$, $i = 1, \dots, N_A^{RF}$ of $\boldsymbol{F}_A$ are chosen from a predefined, finite set of vectors $\mathcal{C}_A$, which we will henceforth call the codebook. The codebook $\mathcal{C}_A$ is a hierarchical codebook with $L_A = \log_2(N_A/N_A^{RF}) + 1$ levels. Each of the levels comprises a subset $\mathcal{C}_A^{(k)}$, $k = 1, \dots, L_A$ of all vectors in the codebook, fulfilling $\mathcal{C}_A = \bigcup_{k=1}^{L_A} \mathcal{C}_A^{(k)}$ and $\bigcap_{k=1}^{L_A} \mathcal{C}_A^{(k)} = \emptyset$. The sub-codebooks $\mathcal{C}_A^{(k)}$ contain a number of N_A-dimensional column vectors which increases with the level k, and we define the sub-codebook size for the kth level as $M_A^{(k)} = \left| \mathcal{C}_A^{(k)} \right| = N_A^{RF} 2^{k-1}$. With this, we can define the kth level sub-codebook for transceiver A as the set $\mathcal{C}_A^{(k)} = \left\{ \boldsymbol{\varphi}_{A,i}^{(k)} : i = 0, 1, \dots, M_A^{(k)} - 1 \right\}$, with elements given by

$$\boldsymbol{\varphi}_{A,i}^{(k)} = \left[1, e^{-j\psi_{A,i}^{(k)}}, \dots, e^{-j(M_A^{(k)}-1)\psi_{A,i}^{(k)}}, \boldsymbol{0}_{N_A - M_A^{(k)}}^{\mathrm{T}} \right]^{\mathrm{T}} \tag{5}$$

where $\psi_{A,i}^{(k)} = \pi - \pi(2i+1)/M_A^{(k)}$ and $\boldsymbol{0}_N$ denotes the all-zeroes column vector of size N.

The rationale behind this codebook can be understood by inspecting the expression in (5). The vector $\psi_{A,i}^{(k)}$ can be seen as a beamforming vector for a $M_A^{(k)}$-dimensional uniform linear array, which steers the signal in the direction $\arccos(\psi_{A,i}^{(k)}/\pi)$. For a fixed level k, the directional cosines $\psi_{A,i}^{(k)}$, $i = 0, \dots, M_A^{(k)} - 1$ are set to uniformly sample the directional cosine range $[-\pi, \pi]$. As the codebook level k increases, this range is sampled with larger resolution. In addition, as k increases, more antenna elements are used, hence resulting in beamforming vectors with narrower main lobes. An illustration of the directional patterns implemented by the proposed codebook is provided in Fig. 2.

We remark that the optimization of the RF codebooks $\mathcal{C}_A$ and $\mathcal{C}_B$ are not the main focus of this article. For a method allowing for optimizing the RF codebook design subject to quantization constraints we refer the reader to [17].

C. Ping-Pong Beam Training with Hybrid Antenna Arrays

The proposed algorithm for beam training with hybrid arrays is outlined in pseudocode in Algorithm 1.

1) Initialization: At the initialization step, the analog precoders of both devices, $\boldsymbol{F}_A$ and $\boldsymbol{F}_B$, are initialized by setting their columns to all the precoding vectors corresponding to the first level of their respective codebooks. In addition, the baseband precoder of device A, $\boldsymbol{w}_A$, is initialized randomly and normalized to fulfill the unit power constraint of the effective precoder.

2) Ping-Pong Iterations: After initialization, devices A and B start a series of alternate transmissions of training sequences while simultaneously updating their baseband and RF precoders. First, device A transmits a training sequence using the initial precoder settings. Upon reception, device

---

[1]Note that the beamforming gain defined in (4) is directly proportional to the post-processing SNR.

[2]We present here the design of the proposed codebook for device A, while the codebook for transceiver B is defined in an equivalent manner.
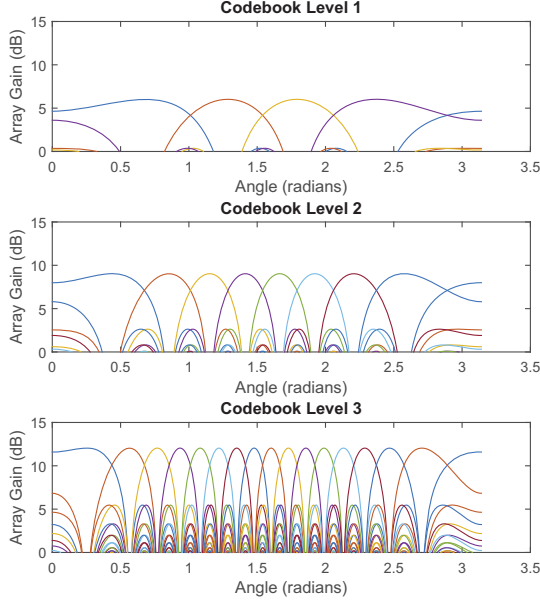
Fig. 2. Array gains obtained with the analog beamformers of the proposed multi-level codebook. $N_A = 16, N_A^{RF} = 4, L_A = 3$.

B obtains an estimate of $\boldsymbol{F}_B^{\mathrm{T}} \boldsymbol{H} \boldsymbol{F}_A \boldsymbol{w}_A$ and sets its digital precoder $\boldsymbol{w}_B$ to the conjugate of the result, following the same procedure as the digital ping-pong beam training method. Immediately after, device B performs a transmission using its newly updated digital precoder. After this transmission, device B updates its RF precoder[3] using the procedure described in lines 20–30 of Algorithm 1, while device A uses the received signal to update its digital precoder. Then, device A performs a transmission with its updated digital precoder. Upon reception, device B conjugates and normalizes the signal, which will be used as its new digital precoder, while device A updates its analog precoders. This completes the first iteration of the ping-pong scheme. The devices continue operating in the same manner for the number of iterations set for beam training.

3) Update of Analog Precoders: The proposed procedure to update the RF precoders requires some further explanation. The update is based on the current state of the device's RF precoder $\boldsymbol{F}$, its codebook $\mathcal{C}$, and the latest update of its baseband precoder $\boldsymbol{w}$, which has entries whose magnitude are proportional to the magnitude of the latest received signal. First, two sequences of values k_n and i_n, $n = 1, \ldots, N^{RF}$ are generated. The value k_n identifies the level of the codebook to which the nth column of the RF precoder belongs; similarly, the value i_n indexes the element within the subcodebook $\mathcal{C}^{(k_n)}$ corresponding to the nth column of $\boldsymbol{F}$. This is, if the nth column of $\boldsymbol{F}$ is equal to the vector $\boldsymbol{\varphi}_{\tilde{i}}^{(\tilde{k})}$ in codebook $\mathcal{C}$, then

[3]The update is performed after transmission in order to keep the equivalent channel $\boldsymbol{F}_B^{\mathrm{T}} \boldsymbol{H} \boldsymbol{F}_A$ seen by the digital processing part constant during a round trip transmission. In this way, each round-trip transmission mimics an iteration of a power iteration algorithm.

Algorithm 1 Ping-Pong Beam Training with Hybrid Arrays

$$\boldsymbol{F}_A^{[0]} \leftarrow \left[\boldsymbol{\varphi}_{A,0}^{(1)}, \boldsymbol{\varphi}_{A,1}^{(1)}, \ldots, \boldsymbol{\varphi}_{A,M_A^{(1)}-1}^{(1)} \right],$$

1: **Initialize:** $\boldsymbol{F}_B^{[0]} \leftarrow \left[\boldsymbol{\varphi}_{B,0}^{(1)}, \boldsymbol{\varphi}_{B,1}^{(1)}, \ldots, \boldsymbol{\varphi}_{B,M_B^{(1)}-1}^{(1)} \right],$

$$\boldsymbol{a} \sim \mathcal{CN}(\boldsymbol{0}_{N_A^{RF}}, \boldsymbol{I}), \boldsymbol{w}_A^{[0]} \leftarrow \frac{\boldsymbol{a}}{\left\| \boldsymbol{F}_A^{[0]} \boldsymbol{a} \right\|_2}.$$

2: A **transmits**.
3: B **receives** $\boldsymbol{y}_B^{[0]} = (\boldsymbol{F}_B^{[0]})^{\mathrm{T}} \boldsymbol{H} \boldsymbol{F}_A^{[0]} \boldsymbol{w}_A^{[0]} + (\boldsymbol{F}_B^{[0]})^{\mathrm{T}} \boldsymbol{n}_B^{[0]}$.
4: $\boldsymbol{w}_B^{[0]} \leftarrow \left(\boldsymbol{y}_B^{[0]} \right)^*$
5: $\boldsymbol{w}_B^{[0]} \leftarrow \frac{\boldsymbol{w}_B^{[0]}}{\left\| \boldsymbol{F}_B^{[0]} \boldsymbol{w}_B^{[0]} \right\|_2}$
6: $t \leftarrow 1$
7: **loop**
8:     B **transmits**.
9:     A **receives** $\boldsymbol{y}_A^{[t]} = (\boldsymbol{F}_A^{[t-1]})^{\mathrm{T}} \boldsymbol{H}^{\mathrm{T}} \boldsymbol{F}_B^{[t-1]} \boldsymbol{w}_B^{[t-1]} + (\boldsymbol{F}_A^{[t-1]})^{\mathrm{T}} \boldsymbol{n}_A^{[t]}$.
10:     $\boldsymbol{w}_A^{[t]} \leftarrow \left(\boldsymbol{y}_A^{[t]} \right)^*$
11:     $\boldsymbol{w}_A^{[t]} \leftarrow \frac{\boldsymbol{w}_A^{[t]}}{\left\| \boldsymbol{F}_A^{[t-1]} \boldsymbol{w}_A^{[t]} \right\|_2}$
12:     $\boldsymbol{F}_B^{[t]} \leftarrow$ UPD. AN. PRECODER$(\boldsymbol{F}_B^{[t-1]}, \boldsymbol{w}_B^{[t-1]}, \mathcal{C}_B)$
13:     A **transmits**.
14:     B **receives** $\boldsymbol{y}_B^{[t]} = (\boldsymbol{F}_B^{[t]})^{\mathrm{T}} \boldsymbol{H} \boldsymbol{F}_A^{[t-1]} \boldsymbol{w}_A^{[t]} + (\boldsymbol{F}_B^{[t]})^{\mathrm{T}} \boldsymbol{n}_B^{[t]}$.
15:     $\boldsymbol{w}_B^{[t]} \leftarrow \left(\boldsymbol{y}_B^{[t]} \right)^*$
16:     $\boldsymbol{w}_B^{[t]} \leftarrow \frac{\boldsymbol{w}_B^{[t]}}{\left\| \boldsymbol{F}_B^{[t]} \boldsymbol{w}_B^{[t]} \right\|_2}$
17:     $\boldsymbol{F}_A^{[t]} \leftarrow$ UPD. AN. PRECODER$(\boldsymbol{F}_A^{[t-1]}, \boldsymbol{w}_A^{[t]}, \mathcal{C}_A)$
18:     $t \leftarrow t + 1$
19: **end loop**

20: **function** UPD. AN. PRECODER$(\boldsymbol{F}, \boldsymbol{w}, \mathcal{C})$
21:     **generate** $k_n, i_n, n = 1, \ldots, N^{RF}$
22:     $v_n \leftarrow |\boldsymbol{w}_n| / \sqrt{M^{(k_n)}}, n = 1, \ldots, N^{RF}$
23:     $n_{\max} \leftarrow \arg \max_n \{v_n : k_n < L\}$
24:     $n_{\min} \leftarrow \arg \min_n \{v_n : n = 1, \ldots, N^{RF}\}$
25:     **if** $n_{\max} \neq n_{\min}$ **then**
26:         **remove** $n_{\max}$th, $n_{\min}$th columns of $\boldsymbol{F}$
27:         **add** new columns $\boldsymbol{\varphi}_{2i_{n_{\max}}}^{(k_{n_{\max}}+1)}, \boldsymbol{\varphi}_{2i_{n_{\max}}+1}^{(k_{n_{\max}}+1)}$ to $\boldsymbol{F}$
28:     **end if**
29:     **return** $\boldsymbol{F}$
30: **end function**

$k_n = \tilde{k}$ and $i_n = \tilde{i}$. Then, the magnitudes of the baseband precoder weights are divided by the square root of the number of array elements active in their corresponding RF chain, producing the sequence v_n, $n = 1, \ldots, N^{RF}$ (line 22). This operation compensates for the fact that RF precoder columns belonging to the different levels of the codebook have different Euclidean norms $\left(\left\| \boldsymbol{\varphi}_i^{(k)} \right\|_2 = \sqrt{M^{(k)}} \right)$. The coefficients v_n will determine which columns of the RF precoder will be updated: first, the index n of the largest coefficient which does not belong to a column in the highest level of the codebook is selected as $n_{\max}$ (line 23); then, the index corresponding to the
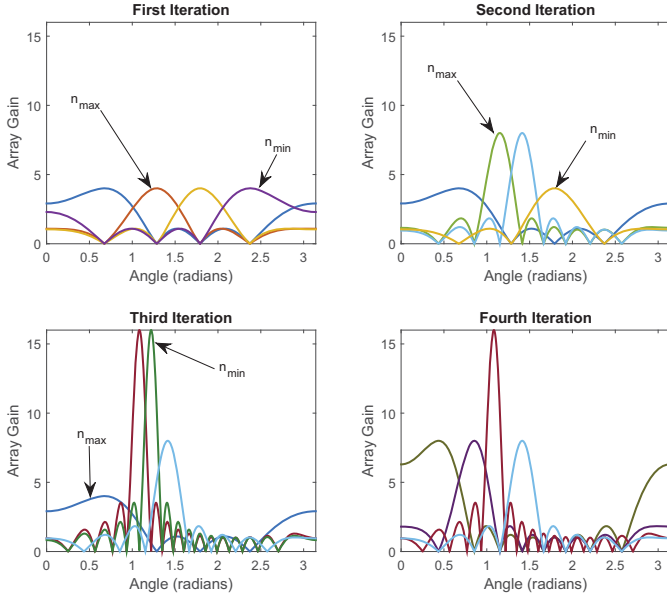
Fig. 3. Illustration of the RF precoder "beam split and drop" update procedure over 4 iterations. $N = 16$, $N^{RF} = 4$, $L = 3$.

Fig. 4. Beamforming gain (dB) attained by the algorithms over a noiseless channel with different number of RF chains. $N_A = N_B = 32$, $P = 5$.

minimum among all coefficients $n_{\min}$ is also selected (line 24). The selected indices correspond to the columns that will be removed from the RF precoder, and to which the "beam split and drop" strategy will be applied. In their place, two vectors from the codebook level immediately above the level corresponding to $n_{\max}$ are included: $\boldsymbol{\varphi}_{2i_{n_{\max}}}^{(k_{n_{\max}}+1)}$ and $\boldsymbol{\varphi}_{2i_{n_{\max}}+1}^{(k_{n_{\max}}+1)}$. With this, the $n_{\max}$th precoder column which was steering the array towards the directional cosine $\psi_{i_{n_{\max}}}^{(k_{n_{\max}})} = \pi - \pi(2i_{\max} + 1)/M_A^{(k_{n_{\max}})}$ is replaced by two columns that steer the array towards the directional cosines $\psi_{2i_{n_{\max}}}^{(k_{n_{\max}}+1)} = \pi - \pi(4i_{n_{\max}}+1)/(2M_A^{(k_{n_{\max}})})$ and $\psi_{2i_{n_{\max}}+1}^{(k_{n_{\max}}+1)} = \pi - \pi(4i_{n_{\max}}+3)/(2M_A^{(k_{n_{\max}})})$, i.e. directional cosines at $\pm\pi/(2M_A^{(k_{n_{\max}})})$ of the original directional cosine $\psi_{i_{n_{\max}}}^{(k_{n_{\max}})}$. As the two new columns added to $\boldsymbol{F}$ belong to an upper level in the codebook than the $n_{\max}$th column, they result in a directional pattern that is twice as directive, steering the array in two directions around the original direction. This update provides better gain and spatial resolution than the original $n_{\max}$th column. The improvement is accomplished at the cost of dropping the $n_{\min}$th precoder column, which had observed the lowest signal among all RF branches. The "split-and-drop" update procedure is illustrated in Fig. 3.

As a result of the update procedure outlined above, Algorithm 1 tends to set the RF precoders to steer the arrays towards the directions where most signal is received with high directivity. Meanwhile, the baseband precoders are set following a power iteration scheme that, with fixed RF precoders $\boldsymbol{F}_A$ and $\boldsymbol{F}_B$, will converge (in the absence of noise) to the max left and right singular vectors of the effective baseband channel $\boldsymbol{F}_B^{\mathrm{T}}\boldsymbol{H}\boldsymbol{F}_A$. Although the algorithm is heuristic, we will show in the coming section that it yields effective precoders that result in a beamforming gain very close to the optimum
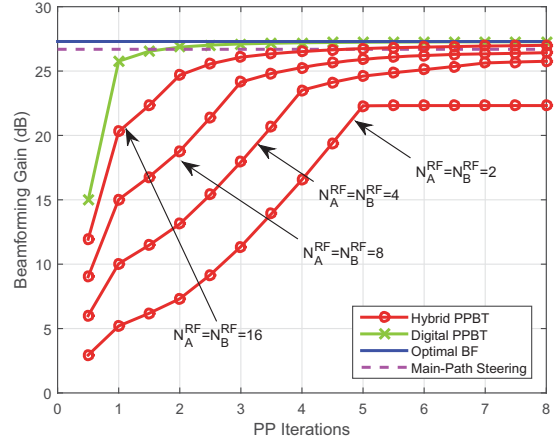
gain G_{opt}, and hence approximates the channel's top singular mode.

IV. PERFORMANCE EVALUATION

We evaluate the performance of the proposed training scheme via Monte Carlo simulations for several configurations of the hybrid array at devices A and B. The channel matrix $\boldsymbol{H}$ is generated according to the model (3), which assumes that the channel response is made of P paths with equal variance and uniformly distributed directions of departure and arrival. The average SNR for the link between the nth element of the array at device B and the mth element of the array at A is defined as $\rho = \mathbb{E}\{|H_{nm}|^2\}/\mathbb{E}\{|n_n^B|^2\} = 1/\sigma^2$, where n_n^B denotes the nth entry of the noise vector $\boldsymbol{n}_B$, H_{nm} is the channel coefficient between the nth and mth elements of arrays B and A and $\mathbb{E}\{\cdot\}$ is the expectation operator.

The performance is measured by means of the average beamforming gain across iterations of the training procedure. For integer iteration t, the beamforming gain is calculated as $(\boldsymbol{w}_B^{[t-1]})^{\mathrm{T}}(\boldsymbol{F}_B^{[t-1]})^{\mathrm{T}}\boldsymbol{H}\boldsymbol{F}_A^{[t-1]}\boldsymbol{w}_A^{[t]}$, while for half integer iteration $(t + 0.5)$ is $(\boldsymbol{w}_B^{[t]})^{\mathrm{T}}(\boldsymbol{F}_B^{[t]})^{\mathrm{T}}\boldsymbol{H}\boldsymbol{F}_A^{[t-1]}\boldsymbol{w}_A^{[t]}$. We benchmark the performance of our proposed training procedure (Hybrid PPBT) against the performance of the digital ping-pong beam training method (Digital PPBT) described in [12], for which the beamforming gain is calculated in an equivalent manner. In addition, we compare with two other ideal beamformers. First, the optimal beamformers (Optimal BF) obtained by using the left and right top singular vectors of $\boldsymbol{H}$, which result in the optimal gain G_{opt}. Second, we compare with beamformers that steers the arrays in the pair of directions of departure and arrival of the multipath components that provides the larges beamforming gain (Main-Path Steering). This bound can be interpreted as the beamforming gain obtained by an ideal beam search procedure with arbitrary spatial resolution and unaffected by noise.

First, we evaluate the performance of the algorithms over a noiseless channel with 5 multipath components, and for hybrid

arrays made of different number of RF chains. The purpose of this experiment is to evaluate the suitability of the analog precoder updating procedure when the training algorithm is not impaired by noise.[4] The results obtained when the two devices are equipped with identical arrays made of $N_A = N_B = 32$ elements and a number of RF chains that varies between 2 and 16 are depicted in Fig. 4. Not surprisingly, the effectiveness of the algorithm increases with the number of RF chains, as the spatial resolution of the initial beamforming setup improves. When using only 2 RF chains, all angular domain is covered by just 2 beams at initialization, which leads to occasionally dropping important signal components in the initial iterations. When using 4 or more RF chains, however, the training algorithm converges to a beamforming gain that is within 2 dB of that of the fully digital array, which in turn converges to the optimal beamforming gain. Convergence is slower when using hybrid arrays than in the digital case, since the training includes updates of both the digital and the analog precoders. Nonetheless, most of the gain is already achieved after only 4 ping-pong iterations.

Next, in Fig. 5 we fix the number of RF chains of both devices to 8, and evaluate the performance of the training algorithm for different SNRs. As expected, the performance of the training algorithm degrades for lower SNRs, both in the digital and the hybrid array cases. An interesting result is that the hybrid array is less sensitive to noise for very low SNRs. The reason for this is that the signal seen in the digital part of the hybrid array has already benefitted from some beamforming gain provided by the analog combiners and, hence, the power iteration performed in the digital part is more robust to noise. This makes the training algorithm especially attractive for communication at high frequencies, e.g. mmWave systems, since the large propagation losses make it likely that low SNRs will be encountered often. At moderate and high SNRs digital PPBT performs better due to the suboptimality of the "beam split and drop" analog updates. Nonetheless, the performance achieved by the algorithm for hybrid arrays is still very close to that of the digital counterpart, although with slower convergence.

As our training scheme has been devised under the assumption of a sparse directional channel with a small number of multipath conponents, we next test the robustness of the approach against channels with richer scattering. First, we evaluate the performance of the training scheme against an increasing number P of channel components in Fig. 6. It is seen that, as P increases, the optimal beamforming gain degrades. This is expected, as in richer scattering conditions the magnitude of the channel's singular values tends to be more evenly distributed and, consequently, the largest eigenvalue's magnitude decreases. A similar effect is seen for the main-path steering gain. The gains obtained by hybrid and digital PPBT degrade with increasing number of paths at the same rate as the bounds for SNRs of -5 dB and
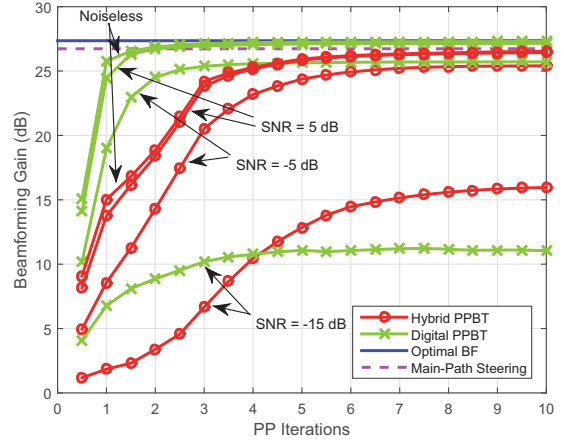
[4]In these conditions, the power iteration implemented by the digital precoder updates converges exactly to the max singular vectors of the analog-beamformed channel.
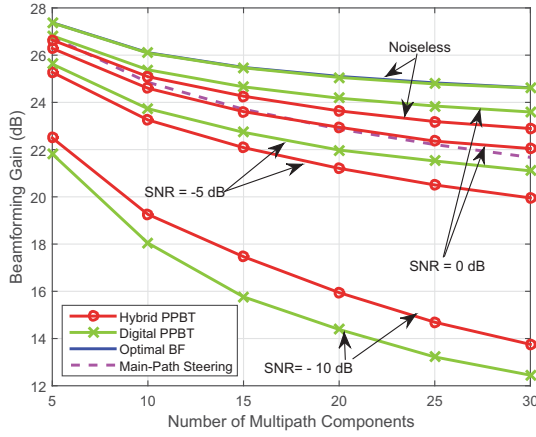

Fig. 5. Beamforming gain (dB) attained by the algorithms over iterations. $N_A = N_B = 32, N_A^{RF} = N_B^{RF} = 8, P = 5$.

above, showing remarkable resilience against rich multipath conditions. In addition, it can be observed that, for SNRs which are large enough, hybrid PPBT outperforms the main-path steering beamformer. This result shows that hybrid PPBT goes beyond the performance of beam search protocols which align all energy in the direction of the main path and, in fact, tries to approximate the top singular mode of the channel. This results from the combination of the "beam split and drop" updates of the analog beamformers with the power iteration performed in the digital part.

To conclude, we evaluate our proposed training procedure in a system in which only one of the devices is equipped with a large, hybrid array ($N_A = 128, N_A^{RF} = 16$), while the other has a full digitally-controlled array of moderate size ($N_B = 8$). In addition, for this case we use an alternative channel model, expressed as

$$H = \frac{\sqrt{N_A N_B}}{P} A_B G A_A^{\mathrm{T}} \tag{6}$$

where A_A contains in its columns the steering vectors $a_A(\Omega_{A,p}), p = 1, 2, \ldots, P$, A_B is defined analogously, P is again the number of multipath components, and G is a $P \times P$ matrix with i.i.d standard complex Gaussian entries. This model reflects the possibility that multipath components are mixed together by the scattering environment, which is more representative of propagation at microwave frequencies [18]. Hence, the presented setup can be interpreted as a massive MIMO system operating at microwave frequencies. As seen by the results shown in Fig. 7, due to the multipath mixing effect there is a larger gap between the beamforming gain obtained with main-path steering and optimal beamforming. As can be seen in the results, the hybrid PPBT scheme convergence is slower than with the channel model (3), but its performance is still very close to optimal for moderate SNRs, and better than the digital counterpart for low SNR. In addition, hybrid PPBT shows again the ability to outperform significantly the main-path steering beamformer. This fact again shows that the

Fig. 6. Beamforming gain (dB) attained with different number of multipath components P. $N_A = 32, N_B = 32, N_A^{RF} = 8, N_B^{RF} = 8$.
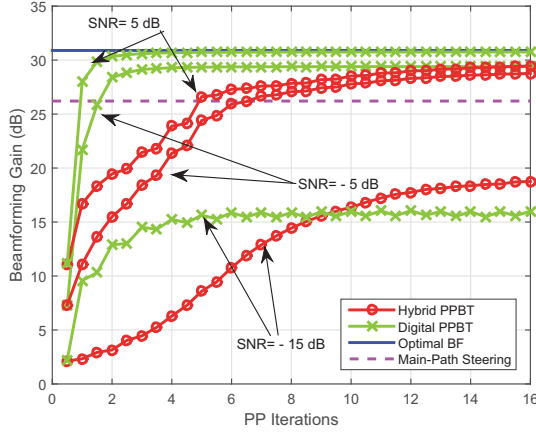

Fig. 7. Beamforming gain (dB) attained by the algorithms over the channel in (6). Device A is equipped with a hybrid array, and device B is equipped with a digital array. $N_A = 128, N_B = 8, N_A^{RF} = 16, P = 5$.

training procedure approximates the top singular of the MIMO channel, rather than just aligning the transmit and receive beamformers in the single directions with largest signal power.

V. CONCLUSION

We have proposed a beam training procedure for devices equipped with hybrid digital-analog antenna arrays, coined hybrid ping-pong beam training. The main virtue of our proposed training is its simplicity, as it involves minimal computational complexity. The procedure relies on an algebraic power iteration method for the setting of the digital precoders, and a codebook search based on a "beam split and drop" strategy in the analog domain. Our results show that the proposed procedure approximates closely the performance of optimal beamforming, given by using the singular vectors of the channel matrix associated to its largest singular value. In addition, the method exhibits great robustness against very low SNR conditions, which makes it especially attractive for

use in mmWave systems. Although some training iterations are needed to achieve near-optimal beamforming, the training procedure can be interleaved with transmission of payload with increasing data-rate. This and the extension to multi-user environments will be the subject of our future research.

REFERENCES

[1] T. S. Rappaport, S. Sun, R. Mayzus, H. Zhao, Y. Azar, K. Wang, G. N. Wong, J. K. Schulz, M. Samimi, and F. Gutierrez, "Millimeter wave mobile communications for 5G cellular: It will work!" *IEEE Access*, vol. 1, 2013.

[2] S. Rangan, T. S. Rappaport, and E. Erkip, "Millimeter wave cellular wireless networks: Potentials and challenges," *Proceedings of the IEEE*, vol. 102, no. 3, pp. 366–385, 2014.

[3] R. W. Heath, N. Gonzalez-Prelcic, S. Rangan, W. Roh, and A. M. Sayeed, "An overview of signal processing techniques for millimeter wave MIMO systems," *IEEE J. Sel. Topics Signal Process.*, vol. 10, no. 3, pp. 436–453, 2016.

[4] X. Zhang, A. F. Molisch, and S.-Y. Kung, "Variable-phase-shift-based RF-baseband codesign for MIMO antenna selection," *IEEE Trans. Signal Process.*, vol. 53, no. 11, pp. 4091–4103, 2005.

[5] V. Venkateswaran and A. van der Veen, "Analog beamforming in MIMO communications with phase shift networks and online channel estimation," *IEEE Trans. Signal Process.*, vol. 58, no. 8, pp. 4131–4143, 2010.

[6] A. Alkhateeb, O. El Ayach, G. Leus, and R. W. Heath, "Channel estimation and hybrid precoding for millimeter wave cellular systems," *IEEE J. Sel. Topics Signal Process.*, vol. 8, no. 5, pp. 831–846, 2014.

[7] J. Lee, G.-T. Gil, and Y. H. Lee, "Exploiting spatial sparsity for estimating channels of hybrid MIMO systems in millimeter wave communications," in *Global Communications Conference (GLOBECOM 2014)*. IEEE, 2014, pp. 3326–3331.

[8] J. Wang, "Beam codebook based beamforming protocol for multi-gbps millimeter-wave WPAN systems," *IEEE J. Sel. Areas Commun.*, vol. 27, no. 8, pp. 1390–1399, 2009.

[9] Y. M. Tsang, A. S. Poon, and S. Addepalli, "Coding the beams: Improving beamforming training in mmwave communication system," in *Global Telecommunications Conference (GLOBECOM 2011)*. IEEE, 2011, pp. 1–6.

[10] J. Andersen, "Transmit-receive diversity in a scattering environment," *COST 259 TD (98)*, Feb 1998.

[11] ——, "Array gain and capacity for known random channels with multiple element arrays at both ends," *IEEE J. Sel. Areas Commun.*, vol. 18, no. 11, pp. 2172–2178, Nov 2000.

[12] E. de Carvalho and J. B. Andersen, "Ping-pong beam training for reciprocal channels with delay spread," in *49th Asilomar Conference on Signals, Systems and Computers*, Nov. 2015, pp. 1752–1756.

[13] T. Dahl, N. Christophersen, and D. Gesbert, "Blind MIMO eigenmode transmission based on the algebraic power method," *IEEE Trans. Signal Process.*, vol. 52, no. 9, pp. 2424–2431, 2004.

[14] H. Ghauch, T. Kim, M. Bengtsson, and M. Skoglund, "Subspace estimation and decomposition for large millimeter-wave MIMO systems," *IEEE J. Sel. Topics Signal Process.*, vol. 10, no. 3, pp. 528–542, 2016.

[15] A. G. Burr, "Capacity bounds and estimates for the finite scatterers MIMO wireless channel," *IEEE J. Sel. Areas Commun.*, vol. 21, no. 5, pp. 812–818, 2003.

[16] G. H. Golub and C. F. Van Loan, *Matrix Computations (3rd Ed.)*. Baltimore, MD, USA: Johns Hopkins University Press, 1996.

[17] S. Payami, M. Shariat, M. Ghoraishi, and M. Dianati, "Effective RF codebook design and channel estimation for millimeter wave communication systems," in *IEEE International Conference on Communication Workshop (ICCW)*, Jun. 2015, pp. 1226–1231.

[18] J. Andersen, "Propagation aspects of MIMO channel modeling," in *Space-Time Wireless Systems*, H. Bolcskei, C. Papadias, D. Gesbert, and A.-J. van der Veen, Eds. Cambridge University Press, 2006, ch. 1.